European Journal of Neuroscience, Vol. 20, pp. 2681–2690, 2004

Input and frequency-specific entrainment of postsynaptic firing by IPSPs of perisomatic or dendritic origin

Gábor Tamás,[1] János Szabadics,[1] Andrea Lörincz[1] and Peter Somogyi[2]
[1]Department of Comparative Physiology, University of Szeged, Közép fasor 52, Szeged H-6726, Hungary
[2]MRC Anatomical Neuropharmacology Unit, University Department of Pharmacology, University of Oxford, Mansfield Road, Oxford OX1 3TH, UK

Abstract

Correlated activity of cortical neurons underlies cognitive processes. Networks of several distinct classes of γ-aminobutyric acid (GABA)ergic interneurons are capable of synchronizing cortical neurons at behaviourally relevant frequencies. Here we show that perisomatic and dendritic GABAergic inputs provided by two classes of GABAergic cells, fast spiking and bitufted interneurons, respectively, entrain the timing of postsynaptic spikes differentially in both pyramidal cells and interneurons at beta and gamma frequencies. Entrainment of pyramidal as well as regular spiking non-pyramidal cells was input site and inhibitory postsynaptic potential frequency dependent. Gamma frequency input from fast spiking cells entrained pyramidal cells on the positive phase of an intrinsic cellular theta oscillation, whereas input from bitufted cells was most effective in gamma frequency entrainment on the negative phase of the theta oscillation. The discharge of regular spiking interneurons was phased at gamma frequency by dendritic input from bitufted cells, but not by perisomatic input from fast spiking cells. Action potentials in fast spiking GABAergic neurons were phased at gamma frequency by both other fast spiking and bitufted cells, regardless of whether the presynaptic GABAergic input was at gamma or beta frequency. The interaction of cell type-specific intrinsic properties and location-selective GABAergic inputs could result in a spatio-temporally regulated synchronization and gating of cortical spike propagation in the network.

Introduction

Neurons of the cerebral cortex communicate by complex temporal and spatial dynamics, but how signals of different frequencies are routed and assessed by cortical networks remains to be explained in terms of specific connections. Electroencephalograms indicate synchronous cortical population activity with dominant frequency components corresponding to particular behaviours (Barlow, 1993; Niedermeyer & Lopes da Silva, 1993). Slow oscillations at about 1–4 Hz are associated with sleep, and rhythms in the beta and gamma frequency bands (15–70 Hz) are typical in the awake states (Steriade *et al*., 1993). Moreover, gamma rhythms are associated with a number of cognitive processes, such as perception and attentional mechanisms (Lisman & Idiart, 1995; Mainen & Sejnowski, 1995; Singer & Gray, 1995; Jefferys *et al*., 1996). Fast network oscillations were proposed to gate the flow of neural information (Salinas & Sejnowski, 2001) and to establish dynamic temporal correlations between spatially distributed neurons, possibly contributing to higher order sensory representations (Singer & Gray, 1995).

Cortical networks have a variety of intrinsic mechanisms that could contribute to synchronous activity (Ritz & Sejnowski, 1997), and γ-aminobutyric acid (GABA)-mediated processes appear prominent in governing rhythmogenesis (Lytton & Sejnowski, 1991; Buzsaki & Chrobak, 1995; Cobb *et al*., 1995; Traub *et al*., 1996; Csicsvari *et al*., 1999; Bartos *et al*., 2001; Wang, 2003). Synchronous, high-frequency firing of putative interneurons has been recorded *in vivo* (Steriade *et al*., 1998; Swadlow *et al*., 1998; Csicsvari *et al*., 1999), and both synaptic and gap junctional coupling can promote synchronous activity in connections of cortical interneurons (Galarreta & Hestrin, 1999; Gibson *et al*., 1999; Koos & Tepper, 1999; Beierlein *et al*., 2000; Tamás *et al*., 2000; Venance *et al*., 2000; Bartos *et al*., 2001). Inhibitory postsynaptic potentials (IPSPs) elicited by some interneuron classes were shown to be highly effective in entraining the firing of postsynaptic neurons (Lytton & Sejnowski, 1991; Cobb *et al*., 1995; Bush & Sejnowski, 1996; Jefferys *et al*., 1996; Bartos *et al*., 2001). Different types of GABAergic cells subdivide the surface of their target neurons (Somogyi *et al*., 1998), and both perisomatically and dendritically terminating populations of interneurons can be synchronized within the same cell class via precise spatiotemporal cooperation of gap junctional coupling with GABAergic synapses (Tamás *et al*., 2000; Szabadics *et al*., 2001). Dendritically and perisomatically terminating cortical interneurons are recruited at characteristic temporal domains during cortical network operations (Klausberger *et al*., 2003, 2004). Cortical GABAergic responses exhibit a wide range of dynamic characteristics, which are determined by both pre- and postsynaptic factors (Gupta *et al*., 2000). Computational models and experiments suggested that the time scale of rhythmic cortical activity could be determined by intrinsic subthreshold membrane potential oscillations and by the decay constant of GABAergic inhibitory synaptic potentials onto the postsynaptic cells (Cobb *et al*., 1995; Traub *et al*., 1996; Hausser & Clark, 1997; Stuart, 1999; Bartos *et al*., 2001; Tiesinga *et al*., 2001). Here we explore how IPSPs evoked by different classes of cortical interneurons entrain postsynaptic firing in distinct types of target cell and how pyramidal cells recruit firing in these interneurons.

Correspondence: Dr G. Tamás, as above.
E-mail: gtamas@bio.u-szeged.hu

Received 28 May 2004, revised 24 August 2004, accepted 25 August 2004

doi:10.1111/j.1460-9568.2004.03719.x

Materials and methods

Electrophysiology and analysis

Slices were obtained from Wistar rats (P18–30) and maintained as described. Animals were anaesthetized with an intraperitoneal injection of ketamine (50 mg/kg) and xilazine (10 mg/kg) and were killed by decapitation. Whole-cell patch-clamp recordings were carried out at ~35 °C from concomitantly recorded pairs, triplets or quadruplets of layer 2–3 putative interneurons and/or pyramidal cells as detailed previously (Tamás *et al*., 2000). Micropipettes (5–7 MW) were filled with (in mM): K-gluconate, 126; KCl, 4; ATP-Mg, 4; GTP-NA2, 0.3; HEPES, 10; creatine phosphate, 10; biocytin, 8 (pH 725; 300 mOsm). Signals were recorded with HEKA EPC9/2 amplifiers in fast current-clamp mode and were filtered at 5 kHz, digitized at 10 kHz and analysed with PULSE software (HEKA, Lambrech/Pfalz, Germany). Presynaptic cells were stimulated with brief (2 ms) suprathreshold pulses at 19 and 37 Hz for the beta and gamma frequency phasing paradigm. Depression/facilitation of IPSPs reaches apparent steady state usually only after 4 or more postsynaptic events; therefore we used 6–11 presynaptic cycles in order to test the effect of the use-dependent modification of IPSPs at two test frequencies on the phasing of postsynaptic activity. We applied the same paradigm throughout the study for consistency. Trains were delivered at >5 s intervals, to minimize intertrial variability. During subthreshold paradigms, postsynaptic cells were held at −50 ± 4 mV membrane potential; traces shown are averages of 30–50 episodes. In order to improve signal-to-noise ratio, pairs were excluded from analysis and phasing experiments if the initial amplitude of compound IPSPs was ≤0.3 mV. This cut-off value excluded similar numbers of presynaptic basket ($n = 24$) and bitufted ($n = 21$) cells from our sample. The investigation of the effect of IPSP amplitude on phasing effectiveness would require a separate study.

For phasing trials, postsynaptic cells were depolarized with constant current injections above threshold so as to elicit firing at 69 ± 30 Hz, without significant differences between types of connections and presynaptic paradigms. Postsynaptic firing probability was evaluated in relation to the presynaptic interspike interval during, prior to and after presynaptic stimulation and was normalized to allow comparison of pairs of a particular type of connection. Friedman's non-parametric repeated measures test was applied to determine significant changes of average firing probability during individual cycles relative to the average of control; consecutive cycles, which were consistently similar to or different from control in all cases of a given type of connection, were grouped. These groups of bins were then compared with one another to validate the grouping relative to control. When all cycles were different from control, bins during presynaptic activity were compared with one another and were grouped accordingly. When no consistent trends were obvious, we split the train of cycles into two groups containing cycles 1–5 and 6–11 at 37 Hz, and 1–3 and 4–6 at 19 Hz. Firing probability plots within such groups of cycles were constructed from 50 to 100 consecutive trials as follows: within the interval separating two presynaptic action potentials, postsynaptic spike latencies were measured from the peak of the preceding presynaptic action potential and binned at 3.375 ms (37 Hz) and 6.5 ms (19 Hz). Controls were collected prior to the onset of the presynaptic spike train using identical cycle duration, and data obtained during presynaptic activation were normalized to control. Friedman's test was used to determine differences relative to control and between bins of different latency in individual presynaptic stimulation cycles. Each bin was compared with the control, then bins were grouped and groups were again compared; if all bins were different from control, we searched for tendencies comparing consecutive bins and/or comparing the bin containing maximal and minimal average firing probability with the rest of bins. Data are given as mean ± SE; differences were accepted as significant at $P \leq 0.05$.

Histology

Visualization of biocytin and correlated light and electron microscopy were performed as described (Tamás *et al*., 2000). Three-dimensional light microscopic reconstructions were carried out using Neurolucida (MicroBrightfield, Colchester, VT, USA) with 100 × objective; dendrogram constructions and synaptic distance measurements were aided by Neuroexplorer (MicroBrightfield) software.

Results

In order to identify the cellular properties underlying the flow of rhythmic activity in the cortex, we have recorded pairs and triplets of interneurons and/or principal cells coupled by GABAergic connections in layers 2–3 of the somatosensory cortex. Following the physiological classification of cell types and their interactions, we analysed the spatial distribution of synapses mediating the interactions. Having identified distinct cell populations and stereotyped arrangement of synapses on the target cells, next we tested some factors that might influence postsynaptic firing behaviour under the influence of rhythmically arriving IPSPs, focusing primarily on the cell type dependence of entrainment and only to a small extent on the underlying mechanisms.

Identification of cell types

According to previously established electrophysiological and anatomical classification of cell types, we have focused our study on the output of fast spiking (*fs*) and bitufted (*bt*) cells innervating *fs*, *bt*, regular spiking non-pyramidal (*rs*) and pyramidal neurons (McCormick *et al*., 1985; Cauli *et al*., 1997; Kawaguchi & Kubota, 1997; Reyes *et al*., 1998; Fig. 1A). In agreement with earlier studies, input resistance and membrane time constant were, on average, 211 ± 36 MΩ and 26 ± 6 ms in pyramidal cells ($n = 23$), 112 ± 28 MΩ and 7 ± 1 ms in *fs* ($n = 44$) cells, 282 ± 54 MΩ and 26 ± 7 ms in *bt* ($n = 40$) and 306 ± 94 MΩ and 23 ± 11 ms in *rs* ($n = 16$) neurons. Similarly to previously determined properties of excitatory postsynaptic potentials (EPSPs) targeting cortical interneurons (Reyes *et al*., 1998; Szabadics *et al*., 2001), unitary input from neighbouring pyramidal cells showed paired-pulse depression on *fs* ($n = 8$, to 58 ± 248%) and *rs* ($n = 26$, 49 and 56%) cells and paired-pulse facilitation on bt ($n = 9$, 232 ± 108%) cells at a paired-pulse interval of 60 ms. Based on intrinsic membrane and firing characteristics and the facilitatory EPSPs received, the *bt* cell class of this study is similar to that of bitufted cells defined by Reyes *et al*. (1998) and to the regular spiking non-pyramidal-somatostatin cell type in Kawaguchi & Kubota (1997) and Cauli *et al*. (2000), and to the low-threshold spiking cells characterized earlier (Gibson *et al*., 1999).

Spatial arrangement of the input from fs and bt interneurons on the target cells

One of the emerging principles of cortical circuitry is the spatial specificity of GABAergic cells (Szentagothai & Arbib, 1974; Kawaguchi & Kubota, 1997; Somogyi *et al*., 1998). We searched

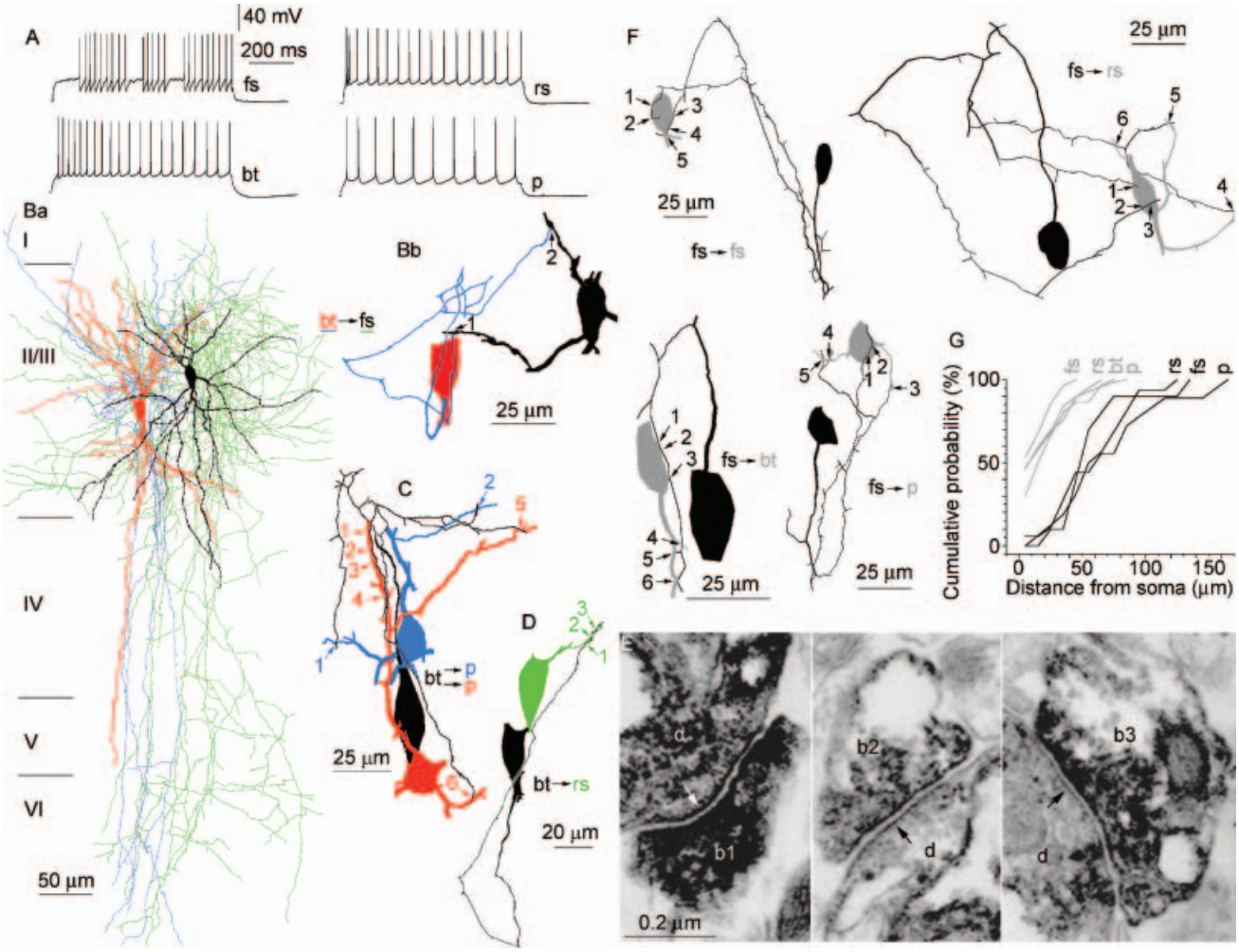

FIG. 1. Pre- and postsynaptic cell types and anatomical analysis of their connections. (A) Firing pattern of fast spiking cells (*fs*), bitufted cells (*bt*), regular spiking non-pyramidal cells (*rs*) and pyramidal cells (*p*). (B–E) Dendritic innervation of distinct types of postsynaptic neuron by *bt* cells. (Ba) Light microscopic reconstruction of a *bt* cell (soma and dendrites, red; axon, blue) to *fs* cell (soma and dendrites, black; axon, green) connection with cortical layers indicated on the left. (Bb) The path of presynaptic axon to the electron microscopically verified synaptic sites (1, 2) of interaction. (C and D) Exclusively dendritic innervation of two pyramidal cells (B, red and blue) and a regular spiking non-pyramidal cell (D, green) by *bt* cells (black). Only presynaptic axons and postsynaptic dendrites forming synapses are represented for clarity. (E) Electron microscopic evidence for three synaptic junctions (arrows) between presynaptic boutons (b1–b3) and the postsynaptic dendrite (d) shown in C. (F) Perisomatic innervation of *fs*, *rs*, pyramidal and *bt* cells (grey) by *fs* basket cells (black). Only synaptically connected axonal and somato-dendritic compartments are shown for clarity. (G) Spatial distribution of identified synapses originating from *fs* basket cells (grey) and *bt* cells (black) on different postsynaptic cells. From each of the seven classes of connection, five cell pairs were selected for light and electron microscopic analysis.

for potential differences in the spatial arrangements of connections between GABAergic cells and from GABAergic cells to pyramidal cells. We assessed the number and position of synapses mediating the interactions by correlated light and electron microscopy (Fig. 1B–G). From each class of connection tested for postsynaptic spike timing, five cell pairs were selected for light microscopic mapping of connectivity; the selection was based on the relative completeness of the presynaptic axonal and postsynaptic dendritic trees from the classes in which we had more than five examples. Of these, full electron microscopic evaluation of predicted synapses was performed in 11 pairs, including all classes of connections. In addition, in the rest of the selected pairs, somata ($n = 16$) postsynaptic to *fs* cells were completely examined in serial ultrathin sections to avoid the light microscopic underestimation of the number of synapses targeting the cell body. Both *fs* and *bt* cells innervated postsynaptic neurons through similar numbers of synapses (5 ± 2 and 3 ± 2, respectively). However, the subcellular positions of synapses formed by *fs* and *bt* cells were significantly different ($P \leq 0.02$; Mann–Whitney *U*-test), regardless of the type of target neuron. The *fs* cells innervated the soma and proximal dendrites of the postsynaptic neurons (20 ± 16 µm from the soma, including synapses on the soma); therefore we identify these cells as basket cells. In contrast, more distal dendrites were innervated by *bt* cell synapses, which were on average 65 ± 25 µm from the soma.

Connection-dependent efficacy of single IPSPs in phasing postsynaptic action potentials

Given the spatial separation of GABAergic inputs on the surface of postsynaptic cells in our sample, we tested whether a solitary IPSP could reset the phase of rhythmic firing evoked by depolarization in interneurons, following reports that in pyramidal cells rhythmic firing was phase-locked by a single IPSP (Cobb *et al.*, 1995; Miles *et al.*, 1996; Stuart, 1999; Gupta *et al.*, 2000). We recorded single IPSPs in *fs* cells evoked by different types of presynaptic cells (*fs*, $n = 3$; *bt*, $n = 6$) on the perisomatic and dendritic domain, but having similar

decay time constants recorded at the soma (20 ± 10 ms and 17 ± 10 ms, respectively). Solitary IPSPs elicited either by *fs* cells or *bt* cells could phase-lock the firing of the postsynaptic *fs* cells to the IPSP at frequencies of 27 ± 6 Hz for up to three successive cycles (Fig. 2A). We have also found that a single IPSP elicited perisomatically by *fs* ($n = 4$) or dendritically by *bt* ($n = 5$) cells phase-locked postsynaptic pyramidal cell firing at theta frequency for two–three consecutive cycles (not shown).

The kinetics of IPSPs differ between cell types and may also differ between distinct inputs to the same cell. The duration of somatically detected IPSPs may also constrain rhythmic firing. We searched for kinetically distinct IPSPs targeting the same postsynaptic cell type, and found them reproducibly in one of the interneuron types in our sample, the *rs* cell (Fig. 2B). Interestingly, IPSPs elicited dendritically by *bt* cells had faster rise and decay characteristics than those evoked by *fs* cells around the soma. Averaged IPSPs elicited by single presynaptic spikes of *fs* ($n = 5$) or *bt* ($n = 5$) cells in *rs* cells had 10–90% rise times of 15.2 ± 8.5 ms and 4.4 ± 0.5 ms, respectively ($P \leq 0.05$, Mann–Whitney *U*-test) and decay times of 88 ± 29 ms and 27 ± 9 ms ($P \leq 0.001$). The firing of postsynaptic *rs* cells was decreased for 62 ± 11 ms by *fs* cells, and for 31 ± 7 ms by *bt* cells ($P \leq 0.01$; bin width, 13 ms, Fig. 1C). These results demonstrate that the duration of IPSPs contributes to the period of altered firing in the same type of cell. In *rs* cells, however, postsynaptic firing did not show significant periodicity before or after a single IPSP.

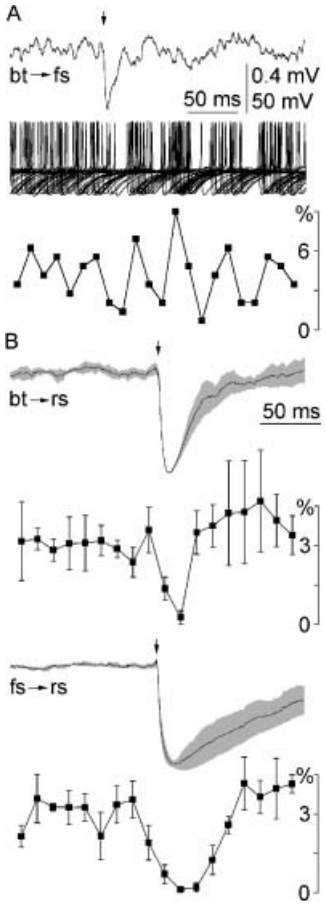

FIG. 2. Connection-dependent efficacy of single IPSPs in phasing postsynaptic action potentials. (A) Prolonged modulation of postsynaptic firing by a single IPSP. An IPSP (top) evoked in a *fs* cell by action potentials of a *bt* cell (arrow marks time of presynaptic spike) reset rhythmic firing in the depolarized postsynaptic *fs* cell for up to three successive cycles at beta frequency (middle, 32 superimposed sweeps aligned on the presynaptic spike). Bottom, firing probability plot of the *fs* cell (13 ms bin width). (B) The time course of the IPSPs influences the return of postsynaptic firing in some cell types. Top, average time course of normalized IPSPs evoked in *rs* cells by single action potentials (arrow marks time of presynaptic spike) of *fs* ($n = 5$) and *bt* ($n = 5$) cells. Bottom, corresponding average firing probability distributions of postsynaptic *rs* cells.

Timing of postsynaptic action potentials by differentially placed compound IPSPs

Because many interneurons fire repeatedly at high frequency *in vivo* (Steriade *et al.*, 1993; Swadlow *et al.*, 1998; Csicsvari *et al.*, 1999; Klausberger *et al.*, 2003), we systematically measured the efficacy of GABAergic inputs at beta and gamma frequency on setting the phase of postsynaptic action potentials in three types of target neuron. The method of quantitative evaluation of action potential timing during different periods of rhythmic presynaptic GABAergic inputs is shown in Fig. 3A–C in an example of a *fs* cell to *fs* cell connection. Presynaptic cells were stimulated with trains of action potentials at gamma (37 Hz) and beta (19 Hz) frequency, and compound unitary IPSPs were recorded postsynaptically. Then, postsynaptic cells were depolarized above threshold to characterize the effect of the same unitary IPSP series on influencing the timing of postsynaptic spikes. Cortical rhythmic activity at higher frequencies is often nested in slower ongoing oscillations (Buzsaki & Chrobak, 1995; Ritz & Sejnowski, 1997; McBain & Fisahn, 2001; Wang, 2003); therefore, when observed, we analysed postsynaptic firing according to different phases of ongoing membrane behaviour as detected in separate subthreshold paradigms (see Materials and methods). In order to reduce the number of variables, comparisons were made between IPSPs having similar ($P > 0.05$) somatically recorded amplitudes. To test input specificity, IPSPs evoked by terminals in either the somatic/perisomatic or the more distal dendritic domain of the postsynaptic target cells were compared. Electrical and combined electrical and GABAergic interactions between cells were not included in this paper because in-depth analysis of all permutations would result in an exceedingly large and complex data set.

Input to fs cells

First we compared the effect of GABAergic input from *fs* and *bt* cells on *fs* cells (Fig. 3D–G). Postsynaptic *fs* cells responded with unitary IPSPs of decremental amplitude to trains of action potentials elicited at beta and gamma frequency (19 and 37 Hz, respectively) in either of the two presynaptic cell types. The initial amplitudes of *fs* to *fs* and *bt* to *fs* IPSPs were similar and decreased to approximately 28–49% of the first response regardless of the source of the input. Presynaptic spike trains of *bt* cells at beta and gamma frequencies moderately decreased the mean frequency of depolarization-evoked postsynaptic firing in *fs* cells to 85 ± 13% and 80 ± 14% of the control values, respectively; input from *fs* cells had a variable effect on the average rate of firing in *fs* cells. In two pairs the firing rate of the postsynaptic cell was unaffected; in three postsynaptic cells it was reduced. As a result of this variability, the average rate of firing in *fs* cells was not reduced significantly (Fig. 3D). Postsynaptic firing rate remained relatively stable during presynaptic cell activation when comparing the averages during individual cycles, showing that postsynaptic *fs* cells were not rhythmically entrained at frequencies lower than the applied test frequencies. However, postsynaptic *fs* cell firing was entrained within each cycle for the entire duration of presynaptic activation. After the preceding presynaptic spike, gamma frequency GABAergic inputs from both *fs* and *bt* cells significantly decreased the probability

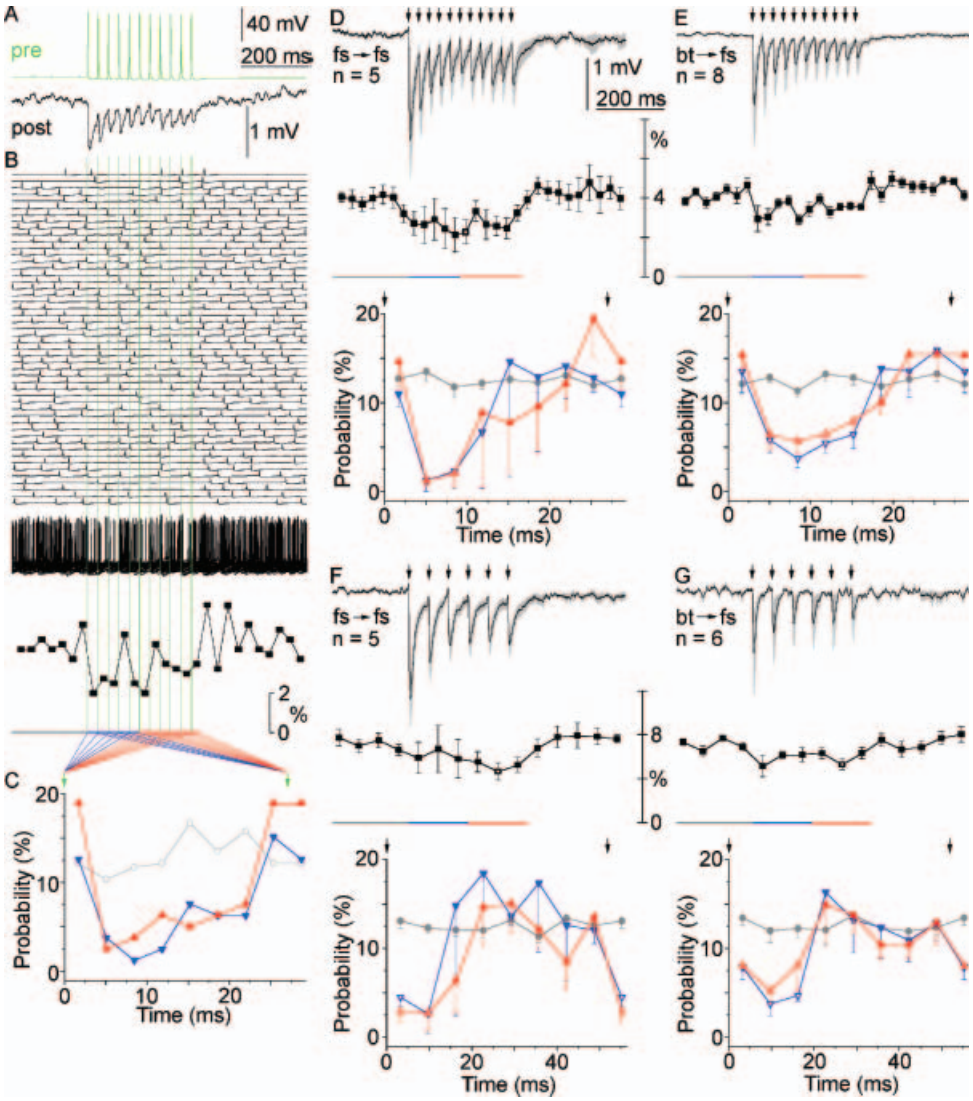

FIG. 3. Similar influence of gamma and beta frequency presynaptic GABAergic activity of two different sources on *fs* cells. (A–C) Analysis of the efficacy of a unitary connection (*fs* to *fs* cell example) in phasing the firing of the postsynaptic neuron by presynaptic firing. Repetitive presynaptic activation (top, 37 Hz) and postsynaptic subthreshold response (bottom). (B) Top, 50 consecutive sweeps from the activity of a tonically depolarized postsynaptic cell during repeating the presynaptic regime. Middle, superimposition of the 50 sweeps. Bottom, firing probability plot of the postsynaptic cell (the bin width corresponds to the length of a single presynaptic cycle). (C) Distributions of postsynaptic firing probability during a presynaptic action potential cycle (arrows) averaged during the control period (prior to the onset of presynaptic firing, grey), the first five (blue) and the last six (red) cycles. (D and E) Top, repetitive presynaptic firing at 37 Hz (arrows) in *fs* (D) and *bt* (E) cells resulted in unitary IPSPs of decremental amplitude in the postsynaptic *fs* cells (black, average; grey, SD). Middle, normalized firing probability plots of postsynaptic firing of tonically depolarized *fs* cells. Bottom, distributions of postsynaptic firing probability during presynaptic action potential cycles (arrows) averaged during the control period (grey), the first five (blue) and last six (red) cycles. Postsynaptic *fs* cells became effectively entrained with a phase-lag of ~ 15–25 ms during presynaptic activity. Empty symbols indicate significant differences relative to control. (F and G) Repeating the experiments shown in D and E at beta frequency (19 Hz) presynaptic activation resulted in decreased postsynaptic *fs* cell firing probability only for the initial 16–22 ms of a cycle.

of postsynaptic *fs* cell firing only for a limited period of time (Fig. 3D and E). Firing probability decreased in *fs* to *fs* cell connections in the second and third bins (3.4–10.1 ms; $P \leq 0.01$), and in *bt* to *fs* cell connections from the second to fifth bins (3.4–16.8 ms; $P \leq 0.01$; Fig. 3D and E). During beta frequency presynaptic activation of either *fs* or *bt* cells, postsynaptic firing probability returned to control levels following the preceding presynaptic spike after the second or third bins (13–19.5 ms; $P \leq 0.05$; Fig. 3F and G). Both 19 and 37 Hz frequency presynaptic activation suppressed *fs* cell firing for similar periods of time corresponding to the cycle length of gamma-band cortical oscillations. Thus, *fs* cells perform a transformation of beta frequency presynaptic input to gamma frequency rebound activation irrespective of the location of the presynaptic input on their somato-dendritic domain.

Input to rs cells

Postsynaptic *rs* cells responded differently to inputs from *fs* and *bt* cells (Fig. 4). The summated amplitude of unitary IPSPs elicited by *fs* cells increased substantially in response to the first two presynaptic action potentials, then declined irrespective of whether presynaptic firing was evoked at gamma or beta frequencies (Fig. 4A and C). On the other hand, repetitive activation of presynaptic *bt* cells evoked IPSPs of relatively stable amplitude. The latter IPSPs had faster rise and decay kinetics, as mentioned previously.

Presynaptic activity of *fs* cells at gamma frequency phased action potentials at theta frequency in postsynaptic *rs* cells in parallel with a rebound depolarization developing in the *rs* cells following the first three IPSPs; postsynaptic firing was strongly suppressed during the first three presynaptic cycles ($P \leq 0.04$), then it returned close to control levels during the fourth–10th cycles and was significantly reduced again during the 11th cycle ($P \leq 0.02$; Fig. 4A). Following the cessation of IPSPs there was strong rebound firing significantly exceeding the control level ($P \leq 0.05$). Such theta frequency entrainment of *rs* cells was not apparent during *fs* cell input at 19 Hz, although postsynaptic firing was reduced during the first cycle ($P \leq 0.02$). The firing of *rs* cells was not entrained at gamma frequency by *fs* cells, as shown by irregular probability distributions of postsynaptic spikes relative to presynaptic cycles of firing (Fig. 4A).

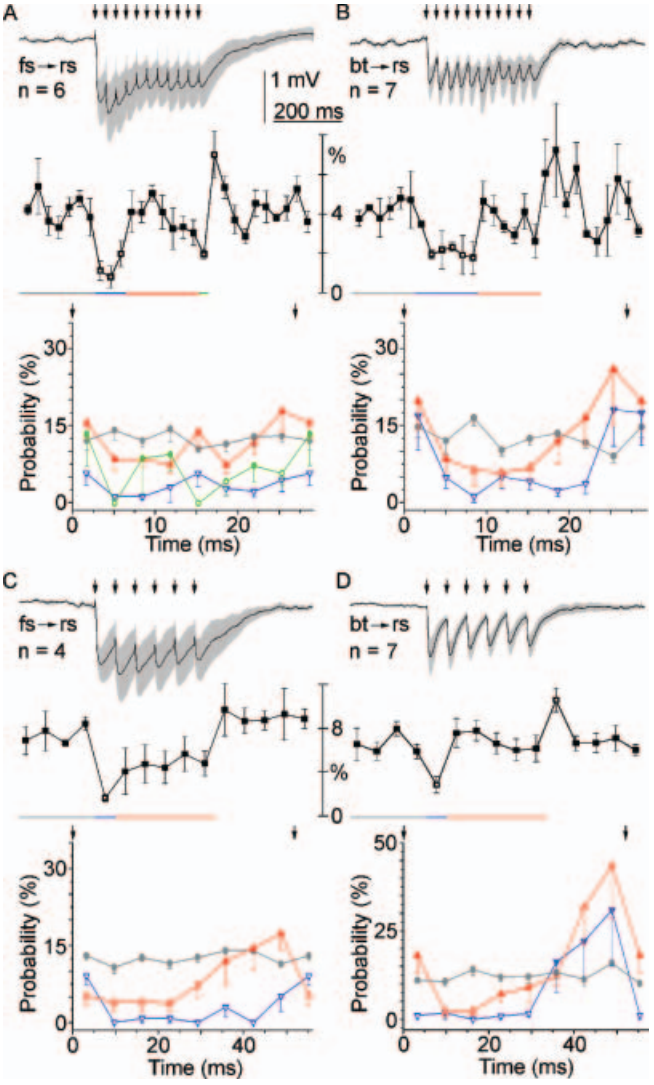

FIG. 4. Differential entrainment of *rs* cell firing by *fs* or *bt* GABAergic inputs. (A) Top, repetitive presynaptic firing at 37 Hz (arrows) in *fs* cells resulted in the summation of unitary IPSPs followed by the stabilization of their amplitude in postsynaptic *rs* cells (black, average; grey, SD). Middle, postsynaptic firing probability plot of tonically depolarized *rs* cells (bin width is equal to the length of a single presynaptic cycle) indicates theta frequency entrainment. Bottom, distributions of postsynaptic firing probability during presynaptic action potential cycles (arrows) averaged during the control period (grey), the first (blue), middle (red) and last three (green) cycles. Gamma frequency phasing did not occur in *fs* to *rs* cell connections. Empty symbols indicate significant differences relative to control. (B) Top, repeating the experiments shown in A between *bt* and *rs* cells. Postsynaptic *rs* neurons responded with unitary IPSPs of stable amplitude and faster decay time constants. Middle, postsynaptic firing was suppressed during the first five presynaptic cycles then returned to the control level. Bottom, distributions of postsynaptic firing probability during presynaptic action potential cycles (arrows) averaged during the control period (grey), the first five (blue) and last six (red) cycles provide evidence for gamma frequency entrainment of *rs* cells by *bt* cells. (C and D) Repeating the experiments shown in A and B with beta frequency (19 Hz) presynaptic activation did not produce entrainment in *fs* to *rs* cell connections, but showed that *bt* cells could phase *rs* cells throughout the entire duration of presynaptic activity.

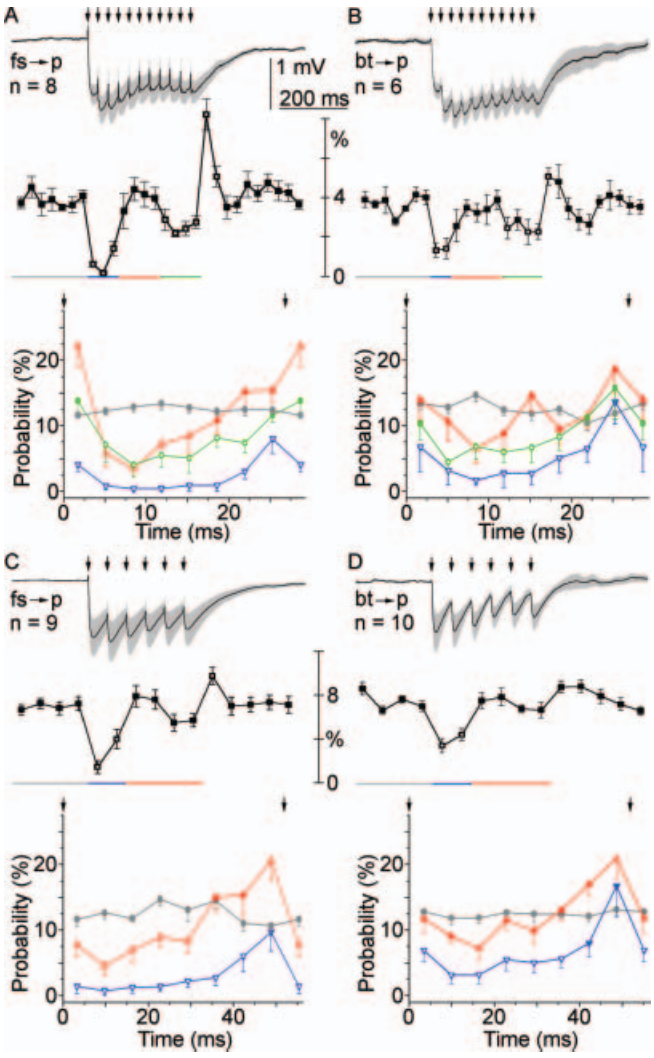

FIG. 5. Differential theta-nested gamma and beta frequency entrainment of pyramidal cell firing by GABAergic inputs from *fs* and *bt* cells. (A and B) Top, repetitive presynaptic firing at 37 Hz (arrows) in *fs* (A) and *bt* (B) cells resulted in the summation of unitary IPSPs followed by the stabilization of their amplitude in postsynaptic pyramidal cells (black, average; grey, SD). Middle, firing probability plots of pyramidal cells (bin width is equal to the length of a single presynaptic cycle) indicate theta frequency rhythmicity in pyramidal cells. Bottom, distributions of postsynaptic firing probability during presynaptic action potential cycles (arrows) averaged during the control period (grey), the first (blue), middle (red) and last three (green) cycles. Gamma frequency entrainment is prominent only in the middle three cycles in *fs* to pyramid, and in the first and last three cycles of *bt* to pyramidal cell connections. Empty symbols indicate significant differences relative to control. (C and D) Repeating the experiments shown in A and B with beta frequency (19 Hz) presynaptic activation produced theta nested beta frequency phasing in both *fs* to pyramid and *bt* to pyramid connections.

At beta frequency, however, *rs* cells were synchronized to *fs* cell activity. Postsynaptic firing probability was higher than in the rest of the bins ($P \leq 0.04$) during the first cycle, and *rs* cells fired below control levels in the first five cycles during the rest of the presynaptic cycles ($P \leq 0.02$).

In contrast to *fs* cells, *bt* cells effectively entrained *rs* cells at gamma and beta frequency throughout the entire duration of presynaptic activity, as shown by the highest postsynaptic firing probabilities around the end of the cycle and by groups of neighbouring bins significantly different from control values ($P \leq 0.05$; Fig. 4B and D bottom panels). The control firing rate of *rs* cells was decreased by *bt* cells during the first five cycles at gamma ($P \leq 0.03$), and during the first cycle at beta frequency ($P \leq 0.02$; Fig. 4B and D middle panels). Low-frequency postsynaptic rhythmicity was not detected by statistical comparison of firing probability of the bins in *rs* cells in response to *bt* cell inputs (Fig. 4B and D).

Input to pyramidal cells

Pyramidal cells were differentially entrained by inputs from *fs* and *bt* cells (Fig. 5), but unlike in *rs* cells, subthreshold responses were similar in amplitude and kinetics to both inputs. Unitary IPSPs showed an initial summation; then the amplitude of the compound response declined to a plateau at 74 ± 12% and 69 ± 19% of the summated amplitude at gamma and beta frequency, respectively, to both fs and bt cells.

Presynaptic activity of *fs* and *bt* cells at gamma frequency phased action potentials at theta frequency in tonically firing pyramidal cells. Postsynaptic firing was strongly suppressed during the first three presynaptic cycles in *fs* to pyramid connections ($P \leq 0.01$) then it returned to control levels during the fourth–seventh cycles and was significantly reduced again during the eighth−11th cycles (Fig. 5A and B). In response to inputs from *bt* cells, firing probability was decreased in pyramidal cells during the first two cycles ($P \leq 0.02$), was around control in the third–seventh cycles and dropped back to below control levels in the eighth, 10th and 11th cycles ($P \leq 0.04$). Although firing probability was not significantly different from control in the ninth cycle ($P \leq 0.17$), there was a significant drop from the seventh to the eighth cycle ($P \leq 0.04$) and between the groups of fourth–seventh and eighth−11th cycles ($P \leq 0.02$), therefore we grouped the eighth−11th cycles. Following the last IPSP in the train, pyramidal cells generated rebound spikes. Presynaptic *fs* and *bt* cell activation at beta frequency reduced pyramidal firing during the first two cycles ($P \leq 0.03$); postsynaptic firing returned in the third cycle and remained similar to control until the end of presynaptic activity (Fig. 5C and D). Thus, gamma frequency IPSPs arriving to pyramidal neurons dendritically or perisomatically reset the phase of ongoing theta oscillations at the onset of postsynaptic response. Successive IPSPs within a train elicited at different frequencies become nested relative to the theta rhythm and their effect on postsynaptic firing can be tested on various phases of ongoing theta oscillations.

The phasing of pyramidal cell action potentials by *fs* and *bt* cells at gamma frequency was dependent on the phases of the simultaneous theta rhythm in firing. The entrainment at gamma frequency by *fs* cells was apparent during the entire length of presynaptic activity. During the first three presynaptic cycles, when pyramidal cell firing was suppressed relative to control, postsynaptic firing probability showed a clear increase in the last bin relative to the rest of the bins ($P \leq 0.004$; Fig. 5A, blue). When pyramidal firing rate increased, phasing was clearly revealed by consecutive series of bins significantly different from control during the fourth–seventh ($P \leq 0.01$) and eighth−11th ($P \leq 0.05$) cycle groups (Fig. 5A, red and green). Comparing the amplitude of gamma frequency entrainment measured as differences of bins having maximal and minimal average firing probabilities showed significant differences between cycle groups representing positive (fourth–seventh) and negative (first–third, eighth−11th) phases of the ongoing theta rhythm. The amplitude of gamma frequency entrainment was about twice as high during the positive phase of the theta oscillation (fourth–seventh cycles; 18.6 ± 8.6%; $P \leq 0.03$) than during the first–third and eighth−11th cycles (7.6 ± 5.8% and 9.7 ± 7.6%). In contrast, entrainment of pyramidal cells by *bt* cells was prominent during the first two and the eighth−11th cycles, the negative phases of the theta oscillation. Consecutive series of bins were significantly different from control during the first two ($P \leq 0.05$) and eighth−11th ($P \leq 0.05$) cycles (Fig. 5B), and the amplitude of the gamma frequency entrainment was similar during these cycles. In response to beta frequency presynaptic spike trains in *fs* and *bt* cells, postsynaptic firing dropped relative to control levels in the first two cycles ($P \leq 0.03$) then returned close to control levels (Fig. 5C and D). Both *fs* and *bt* cells entrained pyramidal neurons at beta frequency as demonstrated by differences in firing probability at the beginning and the end of the cycles ($P \leq 0.05$ and 0.03, respectively), but the degree of entrainment did not appear to change during the duration of presynaptic firing (Fig. 5C and D lower panels).

Input to bt cells

We have searched for GABAergic responses in *bt* neurons to *fs* ($n = 24$) and *bt* ($n = 32$) cell activation, but we could only detect *fs* to *bt* connections ($n = 10$, Fig. 6). These results support earlier data on the lack of chemical synapses between low-threshold spiking cells, which are likely to be equivalent to the *bt* class of the present paper

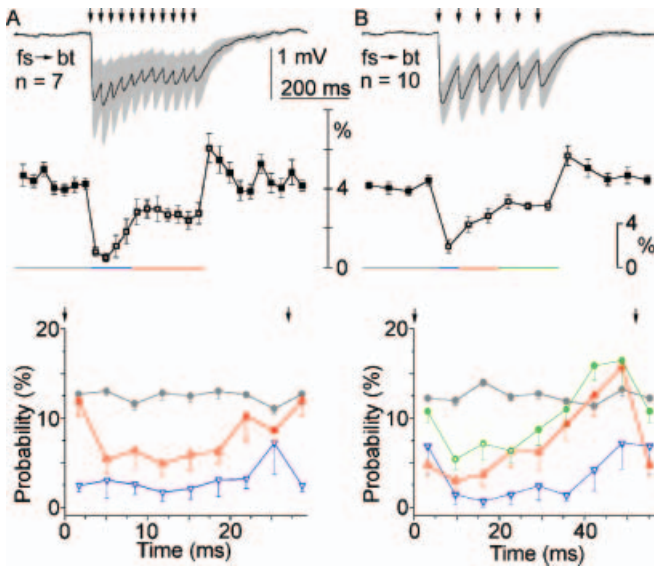

FIG. 6. Frequency-dependent entrainment of *bt* cells by *fs* cells. (A) Top, repetitive presynaptic firing at 37 Hz (arrows) in *fs* cells resulted in the summation of unitary IPSPs followed by the stabilization of their amplitude in postsynaptic *bt* cells (black, average; grey, SD). Middle, firing probability distribution of postsynaptic activity in tonically depolarized *bt* cells (bin width is equal to the duration of a single presynaptic cycle) follows the kinetics of the compound IPSP. Bottom, distributions of postsynaptic firing probability during presynaptic action potential cycles (arrows) averaged during the control period (grey), the first three (blue) and last seven (red) cycles. Gamma frequency phasing occurred only during the last seven cycles. Empty symbols indicate significant differences relative to control. (B) Repeating the experiments shown in A with beta frequency (19 Hz) presynaptic activation showed that *fs* cells could phase *bt* cells throughout the entire duration of presynaptic activity.

(Beierlein *et al.*, 2000, 2003). Bitufted cells responded to gamma frequency input from *fs* cells with compound IPSPs of initially summating, then decrementing, amplitude; the response to beta frequency input was slightly declining throughout. Postsynaptic firing was suppressed relative to control throughout presynaptic activity ($P \leq 0.05$). However, there was a significant increase in firing from the fourth to fifth cycle ($P \leq 0.01$), therefore we grouped cycles accordingly. Entrainment of postsynaptic firing at gamma frequency was clearly defined by consecutive series of bins significantly different from control during the fifth−11th cycles of presynaptic firing ($P \leq 0.03$), but the difference between the minimal and maximal bins was significant during the first four cycles as well ($P \leq 0.04$). Beta frequency presynaptic activation suppressed postsynaptic firing during the entire duration of input ($P \leq 0.05$). Postsynaptic firing showed significant increases from the first to second ($P \leq 0.01$) and from the third to fourth cycle ($P \leq 0.05$), therefore we grouped cycles accordingly. Phasing of *bt* cells was detected during the entire duration of presynaptic *fs* cell activation. The first and eighth bins differed significantly from bins second–sixth during the first presynaptic cycle ($P \leq 0.02$ and $P \leq 0.05$, respectively; Fig. 6B blue). The other bins with suppressed firing relative to control also showed effective beta frequency entrainment in the second–third and fourth–sixth cycles ($P \leq 0.01$ for both cycle groups).

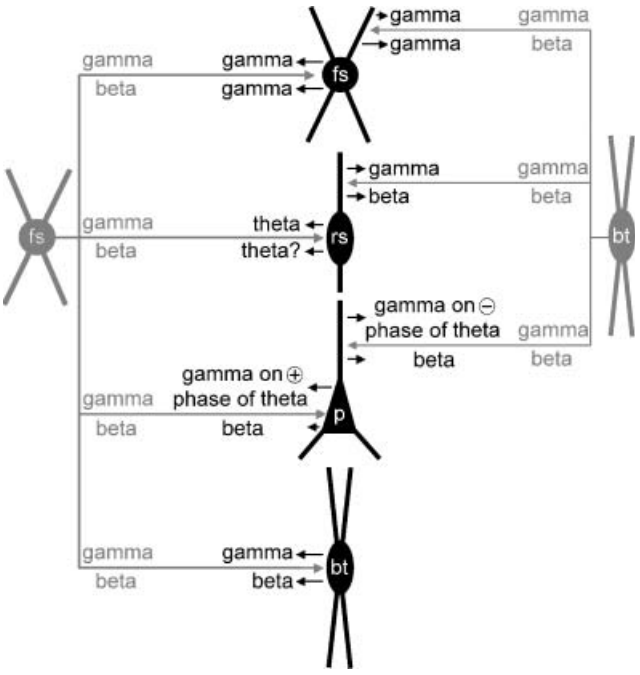

FIG. 7. Input and frequency-specific entrainment of postsynaptic firing by perisomatically and dendritically arriving GABAergic inputs. At least three types of postsynaptic cell (black) receive perisomatic input from *fs* cells and dendritic input from *bt* cells (grey). Beta and gamma frequency inputs, converging onto the same postsynaptic neuron population from *fs* and *bt* cells, are processed differentially. Postsynaptic *fs* cells respond similarly to these two GABAergic inputs; decreased postsynaptic firing probability was detected only for the duration of a gamma cycle. Regular spiking non-pyramidal cells respond differentially to *fs* and *bt* inputs arriving at gamma and beta frequencies; *bt* cells phase *rs* cells at either frequencies, but *rs* cells translate *fs* cell inputs to output at theta frequency. Action potentials of pyramidal neurons are entrained at theta frequency in response to gamma frequency inputs from *fs* and *bt* cells. Moreover, gamma frequency firing entrainment rides on different phases of the theta cycle, depending on the identity of the presynaptic cell, whereas at beta frequency both inputs phase pyramidal neurons continuously. Postsynaptic *bt* cells received inputs only from *fs* cells and their firing was entrained at both gamma and beta frequencies.

Discussion

Entrainment of postsynaptic firing by segregated GABAergic inputs

Our results provide evidence that perisomatic and dendritic GABAergic inputs are capable of entraining several types of postsynaptic neuron in cortical networks (Fig. 7). Entrainment of different non-pyramidal cells by GABAergic afferents might contribute to gamma rhythms, which also arise in mutually interconnected networks of interneurons *in vitro* (Whittington *et al.*, 1995; Fisahn *et al.*, 1998). Electrical coupling through gap junctions is prominent within populations of several classes of GABAergic neuron, including *fs* and *bt* cells studied here, and can promote synchronous activity over a relatively wide range of frequencies (Galarreta & Hestrin, 1999; Gibson *et al.*, 1999; Tamás *et al.*, 2000; Venance *et al.*, 2000; Szabadics *et al.*, 2001). Moreover, precise spatiotemporal cooperation between gap junctional potentials and GABAergic IPSPs is highly effective at synchronizing *fs* and *rs* cells at behaviourally relevant rhythms (Tamás *et al.*, 2000; Szabadics *et al.*, 2001). However, electrical interactions between different classes of interneurons are rare (Gibson *et al.*, 1999; Venance *et al.*, 2000), and only a few experimental studies addressing GABAergic connections between interneurons have tested oscillatory activity systematically (Hausser & Clark, 1997; Bartos *et al.*, 2001).

Contribution of IPSP kinetics to postsynaptic spike timing

Our results show that the kinetics of IPSPs between different classes of interneurons are characteristic to particular connections (see also Gupta *et al.*, 2000; Bartos *et al.*, 2001), and in many cases resulted in an input-dependent entrainment of postsynaptic activity. The similar response of *fs* neurons to inputs from *fs* and *bt* cells resulted in the transformation of beta frequency presynaptic input to a decreased firing probability for only about 20 ms, the duration of one gamma cycle. Therefore, *fs* cells seem to prefer gamma frequency operations (Pike *et al.*, 2000; Fellous *et al.*, 2001) and are likely to be involved in a frequency gating mechanism suppressing slower rhythms. The opposite effect could be observed in connections mediated by the relatively slow IPSPs from *fs* to *rs* neurons, which could not support high-frequency entrainment. Paradoxically, IPSPs elicited on the dendritic domain of *rs* cells were *faster* than perisomatic IPSPs leading to the entrainment of postsynaptic firing in *rs* cells by presynaptic gamma and beta rhythms. Intrinsic, cell type-specific mechanisms, counteracting filtering of dendritic IPSPs and resulting in faster decays than that of the somatic events, might include the local activation of voltage-dependent conductances such as Ih, which might be preferentially expressed on distal dendrites of *rs* cells similar to pyramidal neurons (Magee, 1998). Differences in postsynaptic $GABA_A$ receptors may also contribute to input-specific postsynaptic responses (Pawelzik *et al.*, 1999; Thomson *et al.*, 2000).

Our data support previous results showing that IPSP kinetics and short-term plasticity of unitary IPSPs are influenced both pre- and postsynaptically, and these characteristics are relatively homogeneous in a particular connection (Gupta *et al.*, 2000; Bartos *et al.*, 2001). Similar rules might apply to the entrainment of postsynaptic firing by GABAergic connections, as shown here. However, characteristics of IPSPs are not simply correlated with the efficacy of postsynaptic spike timing, indicating that intrinsic properties of the postsynaptic neurons interact effectively with GABAergic mechanisms in shaping suprathreshold activity. Compound IPSPs showing significant use-depend-

ent depression could lead to theta frequency entrainment in pyramidal and *rs* cells, but no detectable rhythmicity was detected at this frequency band in *fs* cells. In agreement with theoretical and experimental studies (Traub *et al*., 1996; Hausser & Clark, 1997; Magee, 1998; Bartos *et al*., 2001), the decay time constant of IPSPs appears to be an important factor for determining the duration of inhibition of firing, as the fastest decaying IPSPs in *fs* cells resulted in gamma frequency entrainment. However, relatively slower IPSPs were also effective at gamma frequency entrainment in another connection, the *bt* to *rs* cell input. Furthermore, in pyramidal neurons, inputs from *fs* or *bt* cells with similar somatically recorded IPSP kinetics resulted in entrainment with different characteristics in phase-related nesting. Therefore, IPSP kinetics alone do not appear to determine the preferred frequency of entrainment.

Cell type-specific interplay of GABAergic inputs and intrinsic properties in postsynaptic spike timing

We provide evidence that the time course of postsynaptic spiking probability is at least partly determined by the kinetics of the IPSP and, in addition, by intrinsic oscillatory properties of the postsynaptic cells. The preferential response frequency appears to be cell type specific, operating in the theta range in pyramidal cells and at low-range gamma frequencies in *fs* cells, as suggested by experiments injecting sinusoidal currents into different cortical cell types (Pike *et al*., 2000; Fellous *et al*., 2001), and by the rhythmic phase-locked firing after a single IPSP (Cobb *et al*., 1995; Magee, 1999). Cell type specificity of postsynaptic spike timing was further emphasized by reports showing that spike timing also depends on voltage-gated conductances and synaptic background noise (Fellous *et al*., 2003; Schreiber *et al*., 2004).

Moreover, we show here that pyramidal cells can be entrained at frequency ranges above the intrinsic frequency by rhythmically nested GABAergic inputs. Whether similar mechanisms exist in different types of GABAergic neurons is not clear. Further studies will identify the biophysical parameters underlying the cell type-dependent phasing efficacy of somatic vs. dendritic GABAergic inputs. From our results, showing connection-specific spike transmission, it is likely that additional factors determining postsynaptic entrainment are likely to include IPSP or IPSC amplitude, short-term plasticity of inputs and intrinsic properties of the postsynaptic membrane.

Signal combination by theta phase-related nesting of spatially segregated inputs

The synchronized activity of pyramidal neurons is thought to be the basis for population signals recorded in the electroencephalogram (Barlow, 1993; Niedermeyer & Lopes da Silva, 1993). Perisomatically terminating basket and axo-axonic cells phase the activity of postsynaptic pyramidal cells at theta frequency range in the hippocampus *in vitro* (Cobb *et al*., 1995; Miles *et al*., 1996). The present results in the neocortex extend these observations. Firstly, dendritically arriving IPSPs can phase the discharge of pyramidal neurons, similar to *rs* cells reported earlier (Szabadics *et al*., 2001). Secondly, we identify two pathways effective in synchronizing pyramidal cells at gamma frequency operating via perisomatically and dendritically placed GABAergic synapses, respectively. Thirdly, the gamma frequency entrainment by the two inputs is most effective in *two distinct phases* of the simultaneously ongoing theta firing rhythm. The theta phase-related nesting of entrainment by differentially located inputs was only present in pyramidal neurons among the types of postsynaptic cells tested so far. These findings suggest that the firing of pyramidal cells could be especially sensitive to encoding spatial and temporal characteristics of converging GABAergic pathways. Gamma frequency entrainment could promote such a difference, and it is possible that similar mechanisms could be involved in forming an oscillation-dependent combination of signals during cognitive processes (Singer, 1999; Salinas & Sejnowski, 2001).

Connection-specific frequency transformations in the cortical network

We show that the timing of postsynaptic firing in cortical GABAergic connections is highly variable, but also connection specific. The frequency of presynaptic firing may appear to have little influence (e.g. *fs* to *rs*), faithfully followed (*bt* to *rs*), translated to a stereotyped rebound without (*fs* to *fs* and *bt* to *fs*) and with nested intrinsic rhythms (*fs* and *bt* to pyramid) by postsynaptic cells. In the same vein, *fs* cells were entrained similarly by perisomatic and dendritic IPSPs, but action potentials of *rs* and pyramidal cells were timed differentially by similar inputs. Regarding the functional significance of different connections, transformation of rhythmic action potential propagation in *fs* to *fs* and *bt* to *fs* connections suggests a preferential role of *fs* cells in maintaining frequencies in the gamma band (Csicsvari *et al*., 1999; Pike *et al*., 2000; Bartos *et al*., 2001; Destexhe *et al*., 2001). In contrast, the difference in the efficacy of somatic and dendritic inputs in entraining *rs* and pyramidal cells might contribute to the preservation of specificity in the flow of information by gating particular channels at restricted frequencies. Differential theta phase-related entrainment of pyramidal cells by *fs* and *bt* cells could provide a temporal segmentation for readout of multiple input signals (Roelfsema *et al*., 1997; Csicsvari *et al*., 1999). Convergence and divergence of the connections, some identified here for the first time, increase the complexity as well as the computational power of network operations. Connection-specific, spatio-temporally determined spike synchronization might provide a dynamic internal reference in cortical processing in several behaviourally relevant frequency ranges (Singer, 1999; Moore, 2004).

Acknowledgements

The authors thank T. Klausberger for comments on a previous version of the manuscript and E. Tóth for technical assistance. This work was also supported by the Wellcome Trust, the Hungarian Scientific Research Fund (D32815) and the Hungarian Ministry of Education (FKFP 0106/2001). J. Sz. was a Boehringer Ingelheim PhD scholar during part of this project.

Abbreviations

EPSP, excitatory postsynaptic potential; GABA, γ-aminobutyric acid; IPSP, inhibitory postsynaptic potential.

References

Barlow, J.S. (1993) *The Electroencephalogram: its Patterns and Origins.* MIT Press, Cambridge, Massachusetts.

Bartos, M., Vida, I., Frotscher, M., Geiger, J.R.P. & Jonas, P. (2001) Rapid signalling at inhibitory synapses in a dentate gyrus interneuron network. *J. Neurosci.*, **21**, 2687–2698.

Beierlein, M., Gibson, J.R. & Connors, B.W. (2000) A network of electrically coupled interneurons drives synchronized inhibition in neocortex. *Nat. Neurosci.*, **3**, 904–910.

Beierlein, M., Gibson, J.R. & Connors, B.W. (2003) Two dynamically distinct inhibitory networks in layer 4 of the neocortex. *J. Neurophysiol.*, **90**, 2987–3000.

Bush, P. & Sejnowski, T. (1996) Inhibition synchronizes sparsely connected cortical neurons within and between columns in realistic network models. *J. Comp. Neurosci.*, **3**, 91–110.

Buzsaki, G. & Chrobak, J.J. (1995) Temporal structure in spatially organized neuronal ensembles: a role for interneuronal networks. *Curr. Opin. Neurobiol.*, **5**, 504–510.

Cauli, B., Audinat, E., Lambolez, B., Angulo, M.C., Ropert, N., Tsuzuki, K., Hestrin, S. & Rossier, J. (1997) Molecular and physiological diversity of cortical nonpyramidal cells. *J. Neurosci.*, **17**, 3894–3906.

Cauli, B., Porter, J.T., Tsuzuki, K., Lambolez, B., Rossier, J., Quenet, B. & Audinat, E. (2000) Classification of fusiform neocortical interneurons based on unsupervised clustering. *Proc. Natl Acad. Sci. USA*, **97**, 6144–6149.

Cobb, S.R., Buhl, E.H., Halasy, K., Paulsen, O. & Somogyi, P. (1995) Synchronization of neuronal activity in hippocampus by individual GABAergic interneurons. *Nature*, **378**, 75–78.

Csicsvari, J., Hirase, H., Czurko, A., Mamiya, A. & Buzsaki, G. (1999) Oscillatory coupling of hippocampal pyramidal cells and interneurons in the behaving rat. *J. Neurosci.*, **19**, 274–287.

Destexhe, A., Rudolph, M., Fellous, J.M. & Sejnowski, T.J. (2001) Fluctuating synaptic conductances recreate in vivo-like activity in neocortical neurons. *Neuroscience*, **107**, 13–24.

Fellous, J.M., Houweling, A.R., Modi, R.H., Rao, R.P., Tiesinga, P.H. & Sejnowski, T.J. (2001) Frequency dependence of spike timing reliability in cortical pyramidal cells and interneurons. *J. Neurophysiol.*, **85**, 1782–1787.

Fellous, J.M., Rudolph, M., Destexhe, A. & Sejnowski, T.J. (2003) Synaptic background noise controls the input/output characteristics of single cells in an in vitro model of in vivo activity. *Neuroscience*, **122**, 811–829.

Fisahn, A., Pike, F.G., Buhl, E.H. & Paulsen, O. (1998) Cholinergic induction of network oscillations at 40 Hz in the hippocampus in vitro. *Nature*, **394**, 186–189.

Galarreta, M. & Hestrin, S. (1999) A network of fast-spiking cells in the neocortex connected by electrical synapses. *Nature*, **402**, 72–75.

Gibson, J.F., Beierlein, M. & Connors, B.W. (1999) Two networks of electrically coupled inhibitory neurons in neocortex. *Nature*, **402**, 75–79.

Gupta, A., Wang, Y. & Markram, H. (2000) Organizing principles for a diversity of GABAergic interneurons and synapses in the neocortex. *Science*, **287**, 273–278.

Hausser, M. & Clark, B.A. (1997) Tonic synaptic inhibition modulates neuronal output pattern and spatiotemporal synaptic integration. *Neuron*, **19**, 665–678.

Jefferys, J.G.R., Traub, R.D. & Whittington, M.A. (1996) Neuronal networks for induced '40 Hz' rhythms. *Trends Neurosci.*, **19**, 202–208.

Kawaguchi, Y. & Kubota, Y. (1997) GABAergic cell subtypes and their synaptic connections in rat frontal cortex. *Cereb. Cortex*, **7**, 476–486.

Klausberger, T., Magill, P.J., Marton, L.F., Roberts, J.D., Cobden, P.M., Buzsaki, G. & Somogyi, P. (2003) Brain-state- and cell-type-specific firing of hippocampal interneurons in vivo. *Nature*, **421**, 844–848.

Klausberger, T., Marton, L.F., Baude, A., Roberts, J.D., Magill, P.J. & Somogyi, P. (2004) Spike timing of dendrite-targeting bistratified cells during hippocampal network oscillations in vivo. *Nat. Neurosci.*, **7**, 41–47.

Koos, T. & Tepper, J.M. (1999) Inhibitory control of neostriatal projection neurons by GABAergic interneurons. *Nat. Neurosci.*, **2**, 467–472.

Lisman, J.E. & Idiart, M.A.P. (1995) Storage of 7±2 short-term memories in oscillatory subcycles. *Science*, **267**, 1512–1515.

Lytton, W.W. & Sejnowski, T.J. (1991) Simulations of cortical pyramidal neurons synchronized by inhibitory interneurons. *J. Neurophysiol.*, **66**, 1059–1079.

Magee, J.C. (1998) Dendritic hyperpolarization-activated currents modify the integrative properties of hippocampal CA1 pyramidal neurons. *J. Neurosci.*, **18**, 7613–7624.

Mainen, Z.F. & Sejnowski, T.J. (1995) Reliability of spike timing in neocortical neurons. *Science*, **268**, 1503–1506.

McBain, C.J. & Fisahn, A. (2001) Interneurons unbound. *Nat. Rev. Neurosci.*, **2**, 11–23.

McCormick, D.A., Connors, B.W., Lightall, J.W. & Prince, D.A. (1985) Comparative electrophysiology of pyramidal and sparsely spiny stellate neurons of the neocortex. *J. Neurophysiol.*, **54**, 782–806.

Miles, R., Toth, K., Gulyas, A.I., Hajos, N. & Freund, T.F. (1996) Differences between somatic and dendritic inhibition in the hippocampus. *Neuron*, **16**, 816–823.

Moore, C.I. (2004) Frequency-dependent processing in the vibrissa sensory system. *J. Neurophysiol.*, **91**, 2390–2399.

Niedermeyer, E. & Lopes da Silva, F. (1993) *Electroencephalography: Basic Principles, Clinical Applications and Related Fields*. .Williams & Wilkins, Baltimore.

Pawelzik, H., Bannister, A.P., Deuchars, J., Ilia, M. & Thomson, A.M. (1999) Modulation of bistratified cell IPSPs and basket cell IPSPs by pentobarbitone sodium, diazepam and Zn2+: dual recordings in slices of adult rat hippocampus. *Eur. J. Neurosci.*, **11**, 3552–3564.

Pike, F.G., Goddard, R.S., Suckling, J.M., Ganter, P., Kasthuri, N. & Paulsen, O. (2000) Distinct frequency preferences of different types of rat hippocampal neurones in response to oscillatory input currents. *J. Physiol. (Lond.)*, **529 Part 1**, 205–213.

Reyes, A., Lujan, R., Rozov, A., Burnashev, N., Somogyi, P. & Sakmann, B. (1998) Target-cell-specific facilitation and depression in neocortical circuits. *Nat. Neurosci.*, **1**, 279–285.

Ritz, R. & Sejnowski, T.J. (1997) Synchronous oscillatory activity in sensory systems: new vistas on mechanisms. *Curr. Opin. Neurobiol.*, **7**, 536–546.

Roelfsema, P.R., Engel, A.K., Konig, P. & Singer, W. (1997) Visuomotor integration is associated with zero time-lag synchronization among cortical areas. *Nature*, **385**, 157–161.

Salinas, E. & Sejnowski, T.J. (2001) Correlated neuronal activity and the flow of neural information. *Nat. Rev. Neurosci.*, **2**, 539–550.

Schreiber, S., Fellous, J.M., Tiesinga, P. & Sejnowski, T.J. (2004) Influence of ionic conductances on spike timing reliability of cortical neurons for suprathreshold rhythmic inputs. *J. Neurophysiol.*, **91**, 194–205.

Singer, W. (1999) Neuronal synchrony: a versatile code for the definition of relations? *Neuron*, **24**, 49–65.

Singer, W. & Gray, C.M. (1995) Visual feature integration and the temporal correlation hypothesis. *Annu. Rev. Neurosci.*, **18**, 555–586.

Somogyi, P., Tamás, G., Lujan, R. & Buhl, E.H. (1998) Salient features of synaptic organisation in the cerebral cortex. *Brain Res. Rev.*, **26**, 113–135.

Steriade, M., McCormick, D.A. & Sejnowski, T.J. (1993) Thalamocortical oscillations in the sleeping and aroused brain. *Science*, **262**, 679–685.

Steriade, M., Timofeev, I., Durmuller, N. & Grenier, F. (1998) Dynamic properties of corticothalamic neurons and local cortical interneurons generating fast rhythmic (30–40 Hz) spike bursts. *J. Neurophysiol.*, **79**, 483–490.

Stuart, G. (1999) Voltage-activated sodium channels amplify inhibition in neocortical pyramidal neurons. *Nat. Neurosci.*, **2**, 144–150.

Swadlow, H.A., Beloozerova, I.N. & Sirota, M.G. (1998) Sharp, local synchrony among putative feed-forward inhibitory interneurons of rabbit somatosensory cortex. *J. Neurophysiol.*, **79**, 567–582.

Szabadics, J., Lorincz, A. & Tamás, G. (2001) β and γ frequency synchronization by dendritic GABAergic synapses and gap junctions in a network of cortical interneurons. *J. Neurosci.*, **21**, 5824–5831.

Szentagothai, J. & Arbib, M.A. (1974) Conceptual models of neural organization. *Neurosci. Res. Prog. Bull.*, **12**, 305–510.

Tamás, G., Buhl, E.H., Lorincz, A. & Somogyi, P. (2000) Proximally targeted GABAergic synapses and gap junctions synchronize cortical interneurons. *Nat. Neurosci.*, **3**, 366–371.

Thomson, A.M., Bannister, A.P., Hughes, D.I. & Pawelzik, H. (2000) Differential sensitivity to Zolpidem of IPSPs activated by morphologically identified CA1 interneurons in slices of rat hippocampus. *Eur. J. Neurosci.*, **12**, 425–436.

Tiesinga, P.H., Fellous, J.M., Jose, J.V. & Sejnowski, T.J. (2001) Computational model of carbachol-induced delta, theta, and gamma oscillations in the hippocampus. *Hippocampus*, **11**, 251–274.

Traub, R.D., Whittington, M.A., Stanford, I.M. & Jefferys, J.G.R. (1996) A mechanism for generation of long-range synchronous fast oscillations in the cortex. *Nature*, **383**, 621–624.

Venance, L., Rozov, A., Blatow, M., Burnashev, N., Feldmeyer, D. & Monyer, H. (2000) Connexin expression in electrically coupled postnatal rat brain neurons. *Proc. Natl Acad. Sci. USA*, **97**, 10260–10265.

Wang, X.-J. (2003) Neural oscillations. In Nadel, L. (ed.), *Encyclopedia of Cognitive Science*. MacMillan Reference Ltd, Farmington Hills, MI, pp. 272–280.

Whittington, M.A., Traub, R.D. & Jefferys, J.G.R. (1995) Synchronized oscillations in interneuron networks driven by metabotropic glutamate receptor activation. *Nature*, **373**, 612–615.